RAA 2016 Vol. **16** No. **3**, 40 (10pp) doi: 10.1088/1674–4527/16/3/040
http://www.raa-journal.org *http://iopscience.iop.org/raa*

Research in Astronomy and Astrophysics

A magnetic model for low/hard state of black hole binaries

Yong-Chun Ye[1], Ding-Xiong Wang[1], Chang-Yin Huang[2] and Xiao-Feng Cao[3]

[1] School of Physics, Huazhong University of Science and Technology, Wuhan 430074, China; *dxwang@hust.edu.cn*
[2] School of Physics and Optoelectronic Engineering, Yangtze University, Jingzhou 434023, China
[3] School of Physics and Electronic Information, Hubei University of Education, Wuhan 430205, China

Received 2015 April 7; accepted 2015 August 23

Abstract A magnetic model for the low/hard state (LHS) of two black hole X-ray binaries (BHXBs), H1743–322 and GX 339–4, is proposed based on transport of the magnetic field from a companion into an accretion disk around a black hole (BH). This model consists of a truncated thin disk with an inner advection-dominated accretion flow (ADAF). The spectral profiles of the sources are fitted in agreement with the data observed at four different dates corresponding to the rising phase of the LHS. In addition, the association of the LHS with a quasi-steady jet is modeled based on transport of magnetic field, where the Blandford-Znajek (BZ) and Blandford-Payne (BP) processes are invoked to drive the jets from BH and inner ADAF. It turns out that the steep radio/X-ray correlations observed in H1743–322 and GX 339–4 can be interpreted based on our model.

Key words: accretion, accretion disks — black hole physics — magnetic field — stars: individual (H1743–322) — stars: individual (GX 339–4)

1 INTRODUCTION

Although a consensus on classification of spectral states for black hole X-ray binaries (BHXBs) has not been reached, it is widely accepted that these states can be reduced to only two basic cases, i.e., a hard state and a soft state, and jets can be observed in the hard state, but cannot be in the soft one. The accretion flow in the low/hard state (LHS) is usually supposed to be related to a truncated thin disk with an inner advection-dominated accretion flow (ADAF) in the prevailing scenario (Esin et al. 1997, 1998, 2001; McClintock & Remillard 2006; Done et al. 2007; Yuan & Narayan 2014 and references therein). Generally speaking, the thermal component of the spectra of BHXBs can be well fitted by an outer thin disk, while the power law component can be interpreted by an inner ADAF. Although the ADAF model is rather successful in interpreting the spectral state of BHXBs, it has important limitations as pointed out by some authors (e.g., McClintock & Remillard 2006). Besides the power law component being dominant, another feature of LHS of BHXBs is its association with quasi-steady jets. Although the ADAF model is successful in fitting the spectra of LHS of some BHXBs, the details of how the associated jets are produced have not been addressed. Another feature of LHS is that the universal radio–X-ray correlation has been found for a sample of BHXBs (Hannikainen et al. 1998; Corbel et al. 2003; Gallo et al. 2003; Wu & Cao 2006; Wu & Gu 2008; Corbel et al. 2013). However, more and more 'outliers' have been found in recent years, which evidently deviate from the universal radio–X-ray correlation and usually show a much steeper correlation with an index of ~ 1.4 (e.g., H1743–322, Jonker et al. 2010; Coriat et al. 2011; Swift 1753.5-0127, Cadolle Bel et al. 2007; Soleri et al. 2010; XTE J1650-500, Corbel et al. 2004; XTE J1752-223, Ratti et al. 2012).

On the other hand, the most remarkable feature of the state transitions of BHXBs is a phenomenon known as hysteresis, which leads to a counterclockwise q-shaped curve in the hardness-intensity diagram (HID) (Miyamoto et al. 1995; Homan et al. 2001; Fender et al. 2004; Belloni et al. 2005; Homan & Belloni 2005; Fender et al. 2009; Fender & Belloni 2012). However, the hysteresis effect cannot be interpreted by only the accretion rate in the 'one-dimensional' picture of the ADAF model (see Yu & Yan 2009; Kylafis & Belloni 2015).

There is an exception in Cyg X-1 based on the continuous monitoring of Cyg X-1 in the 1.3–200 keV band by using the All-Sky Monitor/Rossi X-Ray Timing Explorer (RXTE) and BATSE/Compton Gamma Ray Observatory for about 200 days from 1996 February 21 to the following early September. It is found that the luminosity of the spectral state transitions in Cyg X-1 is quite constant (Zhang et al. 1997, hereafter ZCH97), thus no q-shaped curve would be seen in HID.

It can be noted that two important discoveries are closely related to the state transitions of X-ray binaries: (i) the correlation between the transition luminosity in the rising phase and the outburst amplitude, which demonstrates that the scale of hysteresis is not arbitrary (Yu et al. 2004);

and (ii) the correlation between the transition luminosity of the state transition in the rising phase and the rate-of-increase of the X-ray luminosity, which supports the hypothesis that the rate-of-change of the mass accretion rate is the apparent second governing parameter (Yu & Yan 2009).

In this paper, we intend to model the LHS of two BHXBs, H1743–322 and GX 339–4, based on the transport of magnetic field into the inner ADAF via the outer thin disk, where the magnetic field is carried by the plasma from the companion. Two promising mechanisms for powering the jet, i.e., the Blandford-Znajek (BZ, Blandford & Znajek 1977) and Blandford-Payne (BP, Blandford & Payne 1982) processes, are invoked for interpreting the association of a quasi-steady jet with LHS. It turns out that the spectral profiles of both BHXBs are fitted in agreement with the data observed at four different dates in the rising phase of the LHS, and the association of the LHS with a quasi-steady jet is satisfied with the steep radio/X-ray correlations for these two sources.

This paper is organized as follows. In Section 2 we give a brief description of our model, and a scenario of the magnetic field being transported with the accreting plasma from the companion is proposed. It is assumed that both accretion rate and magnetic field increase in LHS according to power laws with different indexes. In Section 3 the spectral profiles of LHS of H1743–322 and GX 339–4 are fitted based on the data observed on four different dates in 2003 and 2010, respectively. In Section 4 we fit the radio–X-ray correlation for H1743–322 and GX 339–4; both behave as "outliers" in a power law with much steeper index than the universal correlation. Finally in Section 5, we discuss some issues related to the role of the magnetic field in the state transition of BHXBs.

2 DESCRIPTION OF OUR MODEL

It is widely believed that the most promising mechanisms for powering jets are the BZ and BP processes, which rely on a poloidal, large-scale magnetic field anchored on a spinning black hole (BH) and its surrounding accretion disk (Blandford & Znajek 1977; Blandford & Payne 1982; Livio 2002; Lei et al. 2005, 2008; Wu et al. 2011; Doeleman et al. 2012; Wu et al. 2013; for a review see Spruit 2010). Recently, a number of authors discussed the role of the magnetic field in state transition of BHXBs (Cao 2011; Miller et al. 2012; King et al. 2012; Sikora & Begelman 2013; Dexter et al. 2014). However the origin of the magnetic field in BHXBs remains unclear.

In this paper, we propose a scenario to describe the evolution of the magnetic field associated with outbursts of BHXBs based on the transport of the magnetic field into the accretion disk from the companions. The physical picture of the magnetic field being transported is depicted in Figure 1, and the main features are summarized as follows.

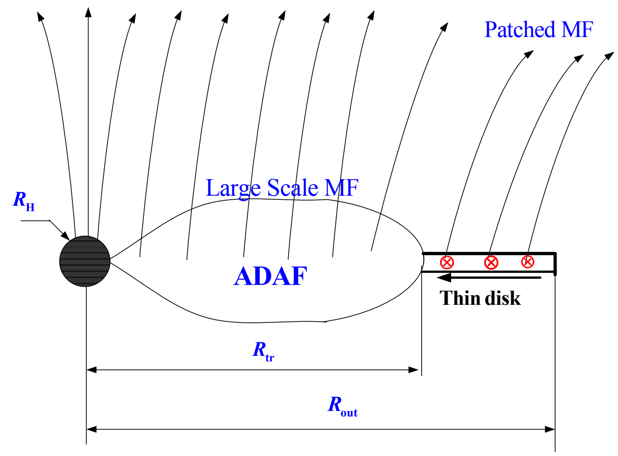

Fig. 1 The large scale magnetic field which is transported to the inner ADAF with the patched fields (represented by the symbol '$\otimes$') being transported through the outer thin disk, which are apt to overcome the magnetic diffusion. The truncated and outer radii of the thin disk are represented by $R_{\rm tr}$ and $R_{\rm out}$, respectively.

(i) The magnetic field is carried by the plasma from the companions and is transported to an accretion disk around a spinning BH.
(ii) The accretion disk consists of two parts, i.e., an inner ADAF and an outer thin disk, between which the truncated radius is $R_{\rm tr}$.
(iii) The relation between a large-scale and a tangled small-scale magnetic field on the disk is given as follows (Livio et al. 1999).

$$B_L \sim (H/R) B_S, \tag{1}$$

where H and R are the half height and disk radius, and B_S and B_L are small- and large-scale magnetic fields on the disk, respectively.

In addition, four assumptions about the transport of a large scale magnetic field are stated as follows.

(i) Patched magnetic fields are assumed to be in the outer thin disk due to MHD turbulence, significantly reducing the outward magnetic diffusion in the thin disk as argued by Spruit & Uzdensky (2005), thus the magnetic field can be transported across the truncated radius.
(ii) The vertical component of the large scale poloidal field maintains the same direction in the inner ADAF during the rising phase of the LHS, as described by a number of authors (Lubow et al. 1994; Spruit & Uzdensky 2005; Igumenshchev 2009; Cao 2011; Guilet & Ogilvie 2013; Sikora & Begelman 2013).
(iii) The strength of the magnetic field at the BH horizon is related to that at the inner ADAF by $B_{\rm H} = 50 B_{\rm ADAF}$ based on results given by Cao (2011), where $R_{\rm H}$ represents the radius of the BH horizon, and $B_{\rm H}$ and $B_{\rm ADAF}$ are the magnetic fields on the BH horizon and ADAF, respectively.

(iv) The contribution of the jet to the X-ray luminosity is distributed uniformly over the whole X-ray band of the spectra of LHS due to lack of a detailed origin for radiation from the jet.

Thus the magnetic flux can be carried by accreting plasma to the ADAF through the truncated thin disk, and the accumulated flux in ADAF is related to the accretion rate as follows.

$$\begin{aligned}\Phi(t) &= \int_{t_b}^{t} \dot{\Phi} dt \\ &= 2^{3/2}\pi\delta^{-1/2}\beta^{1/2}\dot{M}_{\rm Edd}^{1/2}\int_{t_b}^{t}\lambda_{\rm m}^{1/2}(\dot{m}c)^{1/2}cdt. \end{aligned} \quad (2)$$

The quantity $\Phi(t)$ in Equation (2) is the magnetic flux carried by the accreting plasma, and it can be calculated by integrating from t_b to t, which correspond to the beginning of LHS and the subsequent rising phase of LHS, respectively (Fender et al. 2004; Fender & Belloni 2012).

The ratio of magnetic energy density to mass energy density of accreting plasma is defined as $\lambda_{\rm m} \equiv B^2/(8\pi\rho c^2)$, and $\beta = v_{\rm tr}/c$ is the ratio of radial velocity of the accreting plasma at the truncated radius to the speed of light; $\delta = H_{\rm tr}/R_{\rm tr}$ is the ratio of half height to disk radius at the truncated radius. The accretion rate is defined in terms of the Eddington accretion rate, $\dot{m} \equiv \dot{M}/\dot{M}_{\rm Edd}$, which is related to Eddington luminosity by

$$\dot{M}_{\rm Edd} = L_{\rm Edd}/0.1c^2 = 1.4\times10^{18} m_{\rm H}({\rm g\,s^{-1}}), \quad (3)$$

where $m_{\rm H} = M_{\rm H}/M_{\odot}$ is the BH mass in terms of solar mass.

Equation (2) can be easily derived based on the picture of magnetic flux being transported. From Figure 1 and Equation (2) we find that the magnetic flux within the truncated radius $R_{\rm tr}$ can be estimated by

$$\begin{aligned}\Phi_{\rm tr} &= \pi(R_{\rm tr}^2 - R_{\rm H}^2)B_{\rm ADAF} + 2\pi R_{\rm H}^2 B_{\rm H} \\ &= 0.02\pi B_{\rm H}(R_{\rm tr}^2 + 99R_{\rm H}^2),\end{aligned} \quad (4)$$

where $R_{\rm H}$ represents the radius of the BH horizon, and $B_{\rm H}$ and $B_{\rm ADAF}$ are the magnetic fields on the BH horizon and ADAF, respectively. In Equation (4), $B_{\rm H} = 50B_{\rm ADAF}$ is assumed based on the results given by Cao (2011).

In order to discuss the evolution of the magnetic field in LHS we assume that the accretion rate at the truncated radius $R_{\rm tr}$ and the magnetic field at the BH horizon can be expressed as power functions of the outburst time t, i.e.,

$$\dot{m}_{_{R_{\rm tr}}} = \dot{m}_0(t/\tau)^{\alpha_{\rm m}}, \quad (5)$$
$$B_{\rm H} = B_0(t/\tau)^{\alpha_{_B}}, \quad (6)$$

where $\dot{m}_{_{R_{\rm tr}}}$ and $B_{\rm H}$ represent the accretion rate at the truncated radius $R_{\rm tr}$ and the magnetic field at the BH horizon, respectively.

The parameter τ in Equations (5) and (6) is the duration between t_b and the time needed to reach the intermediate state (IMS), going through a rising phase of LHS. We assume $0 \le t/\tau \le 1$ by considering that both $\dot{m}$ and $B_{\rm H}$ attain their maxima $\dot{m}_0$ and B_0 in IMS, respectively. The value of τ varies from several weeks to several months for different BHXBs in different outbursts. Incorporating Equations (4)–(6), we have $R_{\rm tr}$ given by

$$\begin{aligned}R_{\rm tr}^2 = &\ 100\sqrt{2}\delta^{-1/2}\beta^{1/2}c^{3/2}\dot{M}_{\rm Edd}^{1/2} \\ &\tau\frac{\lambda_{\rm m}^{1/2}(t/\tau)^{\alpha_{\rm tr}}}{B_0[(\alpha_{\rm m}/2)+1]} - 99R_{\rm H}^2,\end{aligned} \quad (7)$$

where

$$\alpha_{\rm tr} = (\alpha_{\rm m}/2) - \alpha_{_B} + 1. \quad (8)$$

It is found from Equations (7) and (8) that $\alpha_{\rm tr}$ is related to $\alpha_{\rm m}$ and $\alpha_{_B}$, and the truncated radius $R_{\rm tr}$ increases/decreases with time for positive/negative $\alpha_{\rm tr}$, provided that the values of β, δ, B_0, $\lambda_{\rm m}$ and τ are fixed.

Some authors proposed an excellent description of the general picture of spectral evolutions of BHXBs with the HID. As shown in the HID, LHS is associated with a steady jet with increasing X-ray luminosity, but hardness remains almost unchanged (Fender et al. 2004; Fender & Belloni 2012). As mentioned above, in our model the accretion flow consists of an inner ADAF and an outer thin disk. In order to interpret the association of LHS with quasi-steady jets, we invoke the two most promising mechanisms for powering jets, i.e., the BZ and BP processes, which are closely related to the large scale magnetic fields in the accretion process.

During the past decade both numerical simulations (Stone et al. 1999; Hawley & Balbus 2002; Igumenshchev et al. 2003) and analytical calculations (Narayan & Yi 1994, 1995; Blandford & Begelman 1999; Narayan et al. 2000; Quataert & Gruzinov 2000) have indicated that only a fraction of the plasma accretes onto the BH and the rest is ejected from the outflow. We calculate the global solution of the accretion flow based on an ADAF with a truncated thin disk (e.g., Yuan 2001; Yuan et al. 2005). Then, we solve the radiation hydrodynamics equations self-consistently, obtaining the advection factor $f(r)$ as a function of radius, i.e.,

$$f(r) = q_{\rm adv}/q_{\rm vis} = (q_{\rm vis} - q_{\rm ie})/q_{\rm vis}, \quad (9)$$

where $q_{\rm adv}$, $q_{\rm vis}$ and $q_{\rm ie}$ are the rates of energy advection, viscous heating, and Coulomb collision cooling for the ions, respectively. Meanwhile, Comptonization is treated as a local approximation. The following radiation processes, i.e., bremsstrahlung, synchrotron emission, and the Comptonization of both synchrotron photons from the hot accretion flow and soft photons from the cool disk outside the transition radius are included. The emission from the outer cool disk is modeled as a multicolor blackbody spectrum. The effective temperature as a function of radius is determined by the viscous dissipation and the irradiation of the disk by the inner hot ADAF.

Here, parameters related to the accretion flow are the truncated radius $R_{\rm tr}$, the accretion rate $\dot{m}$, and temperature $T_{\rm tr}$ of the accretion flow at $R_{\rm tr}$ is regarded as an outer boundary condition of the ADAF region (Yuan 1999). In our model, $\dot{m}$ and $R_{\rm tr}$ can be calculated by using Equations (5) and (7), and $T_{\rm tr} = 10^9$ K is taken in a simplified analysis. Furthermore, we take $\alpha = 0.3$ as the "typical" value of the viscosity parameter, and assume that $\sim 10\%$ of the viscous dissipation heats electrons directly. So in our calculations, the free parameters are $\alpha_{\rm m}$, $\alpha_{_B}$ and $\beta_{\rm gas}$, where $\beta_{\rm gas}$ is defined as the ratio of gas pressure to the sum of gas pressure and magnetic pressure. It is found in calculations that $\beta_{\rm gas}$ decreases continuously with time due to the transport of the magnetic field into the inner ADAF.

A number of parameters are involved in our model, and they can be classified into two types based on their roles in the fittings. A summary is given as follows.

Type I: Six free parameters are assigned fixed values before the fittings, i.e., $\dot{m}$, B_0, $\lambda_{\rm m}$, $\alpha_{\rm m}$, β and δ as indicated in Section 3.

Type II: The values of five parameters are determined in the fittings. Specifically, t/τ, $\dot{m}$, $\alpha_{_B}$ and $\beta_{\rm gas}$ are determined in fitting the spectra of H1743–322 and GX 339–4 as shown in Tables 1 and 2 respectively, while those of η_i are determined in fitting the steep radio/X-ray correlations of these two BHXBs by combining the jet contributions described by $L_{\rm R}$ and $L_{\rm X}$ as discussed in Section 4.

All the fittings for H1743–322 and GX 339–4 are based on data observed on four different dates in 2003 and 2010, respectively.

3 FITTING SPECTRAL PROFILES OF LHS OF THE BHXBS

3.1 H1743–322

Now, we fit the spectra of the rising phase of LHS of H1743–322 based on four different observation data, a process which consists of two steps. First, we extract four energy spectra of H1743–322 with observations obtained by the RXTE Proportional Counter Array (PCA) (Obs. ID: 80138-01-01-00; Obs. ID: 80138-01-02-00; Obs. ID: 80138-01-03-00 and Obs. ID: 80138-01-05-00), and set the rising phase of LHS duration of H1743–322 as $\tau = 25~{\rm day} = 2.45 \times 10^6$ s (Joinet et al. 2005; Remillard et al. 2006). Then we can obtain the value t/τ for each date in LHS. Second, combining Equations (5) and (7), we calculate $\dot{m}$ and $R_{\rm tr}$, and fit the LHS spectra of H1743–322 based on the truncated disk model, where $\dot{m}_0 = 0.03$, $\lambda_{\rm m} = 10^{-24}$, $\beta = 0.5$ and $\delta = 1$ are adopted. The BH mass is taken as $M = 10 M_\odot$, the distance to the source as $D = 8$ kpc , and the binary inclination as $\theta = 60°$ (McClintock et al. 2009; Blum et al. 2010; Motta et al. 2010; Coriat et al. 2011). Following Esin et al. (2001) and Yuan et al. (2005), and invoking the formula given by Paczyński (1971), we estimate the outer radius of the truncated thin disk as $R_{\rm out} = 3 \times 10^4 R_{\rm H} (10 M_\odot/M)^{2/3}$.

The fitted spectra of LHS of H1743–322 and the related free parameters are given in Figure 2 and Table 1, respectively. Some authors have pointed out that there is a truncated disk in H1743–322 (e.g., Sriram et al. 2009), and our fitting results for the radius $r_{\rm tr}$ are consistent with their conclusion.

Table 1 The Parameters for Fitting Spectra of LHS for H1743–322 on Four Different Dates

Input						Output
Date	t/τ	$\dot{m}$	$\alpha_{\rm m}$	$\alpha_{_B}$	$\beta_{\rm gas}$	$r_{\rm tr}$
1	0.01	0.003	0.5	0.3	0.86	200
2	0.13	0.011	0.5	1.3	0.82	123.89
3	0.29	0.016	0.5	1.3	0.80	121.43
4	0.45	0.020	0.5	1.3	0.77	120.10

Notes: Dates 1, 2, 3 and 4 in Table 1 indicate 2003 March 26, March 29, April 2 and April 6, respectively. The dimensionless truncated disk radius is defined as $r_{\rm tr} = R_{\rm tr}/R_{\rm H}$.

Table 2 The Parameters Used for Fitting Spectra of LHS of GX 339–4 on Four Different Dates

Date	t/τ	$\dot{m}$	$\alpha_{\rm m}$	$\alpha_{_B}$	$\beta_{\rm gas}$	$r_{\rm tr}$
1	0.01	0.003	0.5	0.3	0.87	300
2	0.12	0.010	0.5	1.3	0.85	250.84
3	0.24	0.015	0.5	1.3	0.84	246.56
4	0.59	0.023	0.5	1.3	0.81	241.00

Notes: Dates 1, 2, 3 and 4 in Table 2 indicate 2010 Jan. 15, Feb. 2, Feb. 15 and March 26, respectively.

3.2 GX 339–4

The steps for fitting GX 339–4 are the same as those for H1743–322. For this source we take the BH mass as $M = 5.8 M_\odot$ (Hynes et al. 2003; Muñoz-Darias et al. 2008), the distance to the source as $D = 8$ kpc (Zdziarski et al. 2004; Hynes et al. 2004), the binary inclination as $\theta = 30°$ (Cowley et al. 2002; Gallo et al. 2004; Miller et al. 2004, 2006, 2009; Reis et al. 2008; Done & Diaz Trigo 2010), and the duration of the rising phase of LHS for GX 339–4 to be $\tau = 110\,{\rm day} = 1 \times 10^7{\rm s}$ (Nandi et al. 2012; Allured et al. 2013). The fitting results and the related parameters are shown in Figure 3 and Table 2, respectively.

Our results show that it is reasonable to assume there is a truncated disk in GX 339–4. The strongest case for disk truncation was presented by Tomsick et al. (2009), in which fluorescent iron emission lines were invoked to find the inner edge of the accretion disk, which is greater than the Schwarzschild radius for GX 339–4 in LHS. Claims of a truncated disk in LHS also appear based on modeling the direct disk emission by accounting for irradiation of the inner disk (Cabanac et al. 2009). Recently, Plant et al. (2014) pointed out that there is a truncated disk in GX 339–4, and it decreases monotonically with time. As shown in Table 2, the variation of the truncated disk of GX 339–4 obtained in our model is consistent with the conclusion given by Plant et al. (2014).

As shown in Table 1 and Table 2, the truncated radii $R_{\rm tr}$ move inward in the rising phase of LHS from 200 to 120.10 and from 300 to 241 corresponding to the varia-

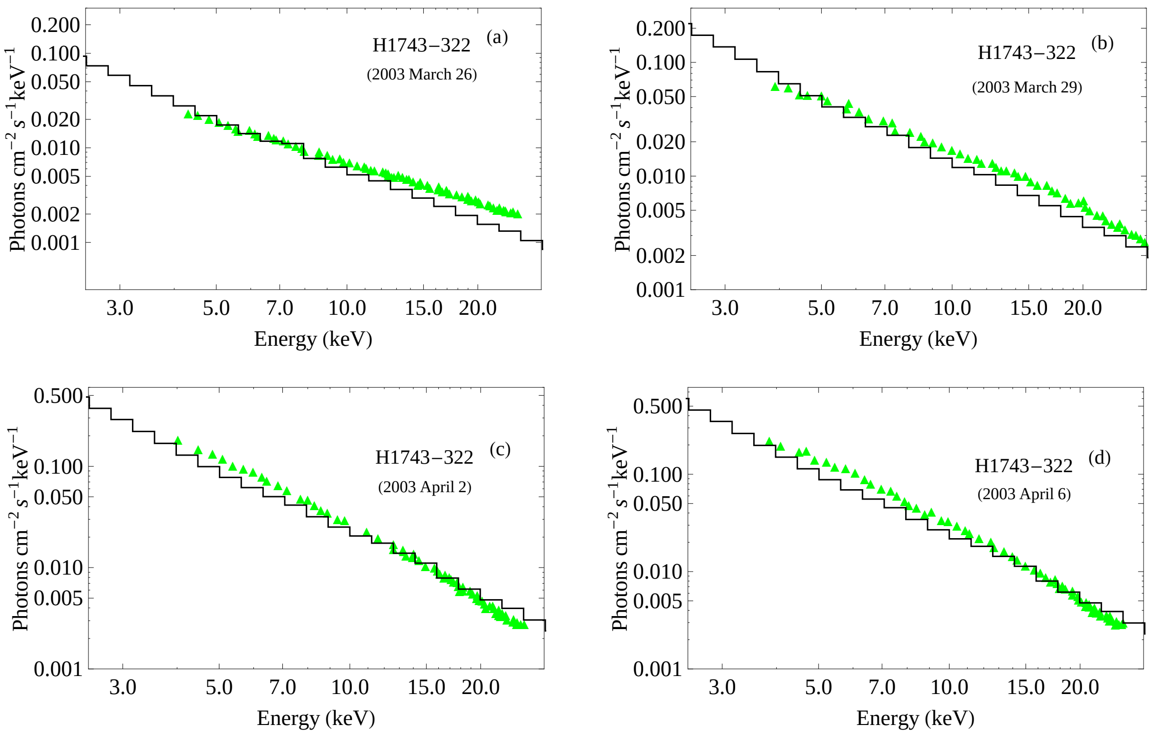

Fig. 2 The spectra of LHS of H1743–322 are represented by jagged lines that are fitted to the green triangles based on the four different dates: (a) 2003 March 26 (Obs. ID: 80138-01-01-00); (b) 2003 March 29 (Obs. ID: 80138-01-02-00); (c) 2003 April 2 (Obs. ID: 80138-01-03-00) and (d) 2003 April 6 (Obs. ID: 80138-01-05-00).

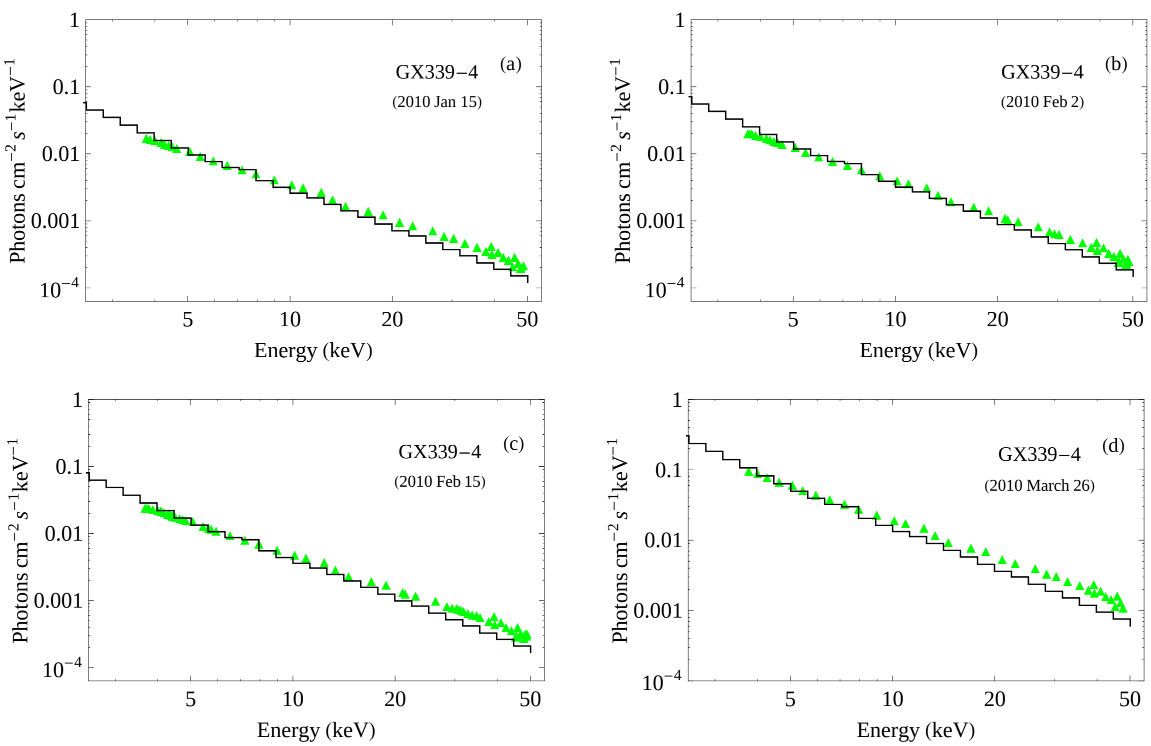

Fig. 3 The spectra of LHS of GX 339–4 are represented by jagged lines that are fitted to the green triangles based on the four different dates: (a) 2010 Jan 15 (Obs. Id: 95409-01-02-02); (b) 2010 Feb 2 (Obs. ID: 95409-01-04-02); (c) 2010 Feb 15 (Obs. ID: 95409-01-06-01) and (d) 2010 March 26 (Obs. Id: 95409-01-12-00).

Table 3 The Parameters for Fitting the Correlation between $L_{\rm R}$ and $L_{\rm X}$ for H1743–322 and GX 339–4 Based on Four Different Observations

Source	Spin	f_0	B_0 (G)
H1743—322	0.2	0.33	7.9×10^8
GX 339–4	0.5	0.33	7.9×10^8

Notes: The spin $a_* = 0.2$ for H1743–322 is taken from Narayan & McClintock (2012), while $a_* = 0.5$ for GX 339–4 is assumed due to lack of data.

tion of accretion rates from 0.003 to 0.020 and from 0.003 to 0.023 for H1743–322 and GX 339–4, respectively. This implies that the large-scale magnetic field becomes progressively more concentrated in the inner ADAF in the rising phase of LHS due to the transport of the magnetic field carried by the accreting plasma. It can also be noted that these values of accretion rates are much less than the critical values, $\sim 0.35 - 0.4$, guaranteeing the validity of the ADAF model in fitting the LHS of these two sources.

4 THE RADIO–X-RAY CORRELATION

The relation between radio luminosity $L_{\rm R}$ and X-ray luminosity $L_{\rm X}$ in LHS of BHXBs has been discussed by a number of authors (Corbel & Fender 2002; Gallo et al. 2003; Fender et al. 2003)

$$L_{\rm R} \propto L_{\rm X}^b, \tag{10}$$

where $b \sim 0.7$ for $L_{\rm X}$ in the 3-9 keV range. However, it has been shown recently that the radio and X-ray emissions of some BHXBs are strongly correlated at high luminosity in LHS with a much steeper power law, i.e., $b \sim 1.4$ in Equation (10), and these sources including H1743–322 and GX 339–4 are referred to as 'outliers' (Jonker et al. 2010; Coriat et al. 2011; Cao et al. 2014).

Very recently, Huang et al. (2014, hereafter HWW14) modeled the steeper radio–X-ray correlation with a slope of 1.2 based on the radiatively efficient disk-corona with the hybrid jet model, in which the radio emission is attributed to the jet with the X-ray emission from the disk corona. Although the steep correlation is fitted to the observed ones in HWW14, the simulated X-ray emission increases more and more slowly and almost becomes saturated at high accretion rates, which may be due to the fact that they did not consider the contribution of the jet to the X-ray radiation. Compared to HWW14, this model focuses on the transport of the magnetic field from the companions in which more attention is paid to the effect of the transport of the magnetic field on the steep correlation in the rising phase of LHS observed in H1743–322 and GX 339–4.

In this paper, the BZ and BP mechanisms are invoked to drive the jet power in LHS of BHXBs, and are considered as follows,

$$L_{\rm J} = P_{\rm BZ} + P_{\rm BP}, \tag{11}$$

where $L_{\rm J}$, $P_{\rm BZ}$ and $P_{\rm BP}$ are the jet power, the BZ power and the BP power, respectively. The BZ power is driven by the spinning BH via the large scale magnetic field on the horizon, and it reads (MacDonald & Thorne 1982; Ghosh & Abramowicz 1997)

$$P_{\rm BZ} = \frac{c}{32}\omega_F^2 B_{\rm H}^2 R_{\rm H}^2 a_*^2, \tag{12}$$

where ω_F is a parameter that relates the angular velocity of the BH to that of the field line on the BH horizon by $\omega_F^2 = \Omega_F(\Omega_{\rm H} - \Omega_F)/\Omega_{\rm H}^2$. The maximum BZ power $P_{\rm BZ}^{\rm max}$ is reached as $\Omega_F = \Omega_{\rm H}/2$, i.e.,

$$\begin{aligned} P_{\rm BZ}^{\rm max} &= \frac{c}{128} B_{\rm H}^2 R_{\rm H}^2 a_*^2 \\ &= \frac{c}{128} B_0^2 R_{\rm H}^2 a_*^2 (t/\tau)^{2\alpha_B}, \end{aligned} \tag{13}$$

where Equation (6) for the evolution of the magnetic field in LHS is used in the last step.

The BP power can be expressed based on our previous work (Li et al. 2010) as follows,

$$P_{\rm BP} = \int_{R_{\rm H}}^{R_{\rm tr}} S_E 4\pi R dR, \tag{14}$$

where $S_E = B_{\rm ADAF}^2 \Omega_{\rm ADAF}^2 R^2/(4\pi c)$ is the energy flux driven in the BP process, and $\Omega_{\rm ADAF}$ is the angular velocity of ADAF, which is related to the Keplerian angular velocity by

$$\Omega_{\rm ADAF} = f\Omega_k, \tag{15}$$

where f is defined as (Narayan & Yi 1994; Yuan et al. 2008, hereafter YMN08)

$$f = \begin{cases} f_0, & \text{for} \quad R \geq 3R_{\rm H}, \\ f_0 3(R - R_{\rm H})/2R, & \qquad R < 3R_{\rm H}. \end{cases} \tag{16}$$

As argued in YMN08, the value of f_0 is taken as 0.33 for all accretion rates as the viscous parameter α is large. Incorporating Equations (6), (13) and (15), we have

$$\begin{aligned} P_{\rm BP} &= \frac{1}{c}\int_{R_{\rm H}}^{3R_{\rm H}} B_{\rm ADAF}^2 \Omega_K^2 (R - R_{\rm H})^2 (9/4) f_0^2 R dR \\ &\quad + \frac{1}{c}\int_{3R_{\rm H}}^{R_t r} B_{\rm ADAF}^2 \Omega_K^2 f_0^2 R^3 dR \\ &= (2 \times 10^{-4} c)(B_0 f_0 R_{\rm H})^2 [(R_{\rm tr}/R_{\rm H}) \\ &\quad -1.95](t/\tau)^{2a_B}. \end{aligned} \tag{17}$$

Combining Equations (12) and (16) we have the ratio of the BZ to BP powers as follows,

$$\begin{aligned} P_{\rm BP}/P_{\rm BZ}^{\rm max} &= (2.56 \times 10^{-2})(f_0/a_*)^2 \\ &\quad \times [(R_{\rm tr}/R_{\rm H}) - 1.95]. \end{aligned} \tag{18}$$

Inspecting Figure 1 and Equations (10) and (17), we find that the ratio of the BZ to BP powers is sensitive to the truncated radius $R_{\rm tr}$ for a fixed BH spin. The contribution to the jet power from the BZ power is roughly equal to that from the BP power, provided that the BH spin is no less that 0.1 with $R_{\rm tr}$ greater than $100R_{\rm H}$. However, the BZ power dominates over the BP power as $R_{\rm tr}$ approaches the

Table 4 The Fractions of Jet Power Converted to X-ray Luminosity Corresponding to Different Observations

H1743–322				GX 339–4			
Date	t/τ	$\dot{m}$	η_i	Date	t/τ	$\dot{m}$	η_i
2003 Mar. 26	0.01	0.003	0.20	2010 Jan. 15	0.01	0.003	0.25
2003 Mar. 29	0.13	0.011	0.23	2010 Feb. 2	0.12	0.010	0.35
2003 Apr. 2	0.29	0.016	0.28	2010 Feb. 15	0.24	0.015	0.39
2003 Apr. 6	0.45	0.020	0.36	2010 Mar. 26	0.59	0.023	0.42

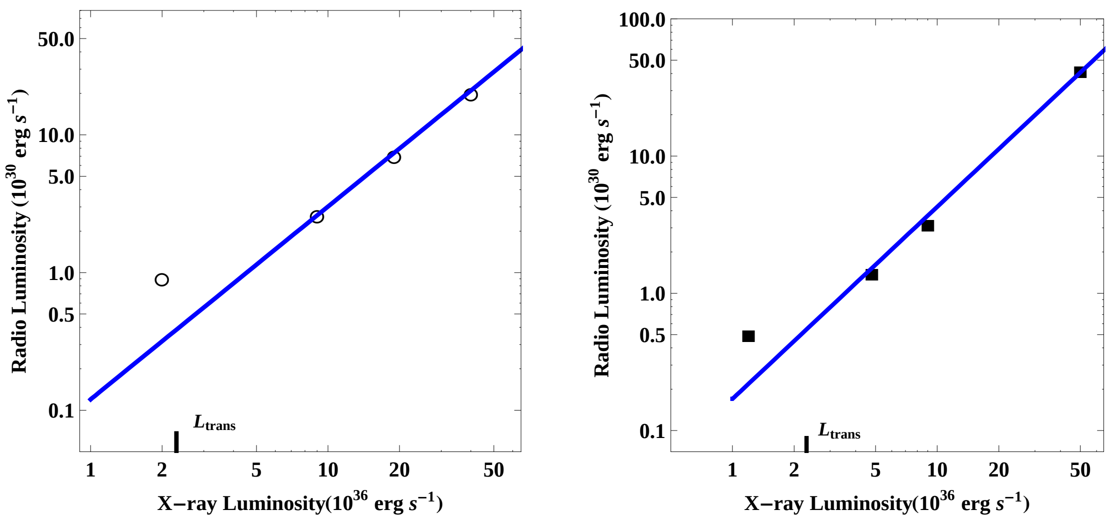

Fig. 4 The radio–X-ray correlations are plotted to fit the observational data based on our model for H1743–322 (*left panel*) and GX 339–4 (*right panel*). The four circles and squares are obtained based on the observations of the rising phase of LHS for H1743–322 and GX 339–4 given in Tables 1 and 2, respectively. The solid lines correspond to the correlation with an index of ~ 1.4.

BH for $R_{\rm tr}/R_{\rm H} \sim 3$. Since the BH spin remains almost unchanged in one outburst of BHXBs, these results imply that the evolution of the magnetic field configuration does play an important role in the state transition from LHS to IMS of BHXBs. We shall discuss this issue in Section 5.

In order to fit the radio–X-ray correlation we should discuss the contribution of the jet power to radio luminosity and X-ray luminosity. Following HWW14 we have the radio luminosity related to the jet power by

$$L_{\rm R} = 6.1 \times 10^{-23} L_{\rm J}^{17/12}\ {\rm erg\ s^{-1}}, \quad (19)$$

where $L_{\rm J}$ can be calculated by combining Equations (11)–(17). Equation (19) is derived by Heinz & Grimm (2005) based on the estimation of jet power for Cyg X-1 and GRS 1915+105. Combining the spectra of LHS and Equation (19) with the values of the input parameters listed in Table 1, we can fit the radio–X-ray correlation for H1743–322 and GX 339–4 by a steep power law index ~ 1.4 as shown in the left and right panels of Figure 4, respectively.

Considering that part of the jet power could be converted to X-ray radiation by some magnetic process, we assume that the radio radiation $L_{\rm R}$ is contributed by a fraction of the BZ and BP powers, and the X-ray radiation $L_{\rm X}$ arises from the sum of the remaining jet power and accretion flow, i.e.,

$$L_{\rm X} = L_{\rm X}^{\rm I} + L_{\rm X}^{\rm II}, \quad (20)$$

where $L_{\rm X}^{\rm II}$ is contributed by accretion flow and $L_{\rm X}^{\rm I}$ is related to the jet power as follows,

$$L_{\rm X}^{\rm I} = \eta_i L_{\rm J}. \quad (21)$$

The parameter $\eta_i (i = 1, 2, 3, 4)$ in Equation (21) is the fraction of the jet power converted to X-ray luminosity corresponding to different observations. It is assumed that the jet contribution is distributed uniformly in the whole X-ray band, and η_i can be determined from fitting the spectra of LHS with the associated $L_{\rm R} - L_{\rm X}$ correlations based on the four observational data of H1743–322 and GX 339–4 as shown in Table 1. It turns out that the steep radio-X-ray correlations can be fitted for H1743–322 and GX 339–4 as shown in Figure 4.

As shown in Figure 4 we have two kinds of radio–X-ray correlations corresponding to (i) from date 1 to date 2 with slopes ~ 0.64 for H1743–322 and ~ 0.63 for GX 339–4; (ii) from date 2 to date 4 with a slope of ~ 1.4. The quantity $L_{\rm trans}$ in Figure 4 is the upper bound of the transition between the two correlations, which is equal to $2.3 \times 10^{36}\ {\rm erg\ s^{-1}}$. These results are consistent with those given by Coriat et al. (2011).

5 DISCUSSION

In this paper, we propose a model to interpret the rising phase of LHS of BHXBs based on the transport of the magnetic field by accreting plasma from the companions. It turns out that the LHS spectra of H1743–322 and GX 339–4 can be fitted separately based on the four different observation data. In addition, the steep radio/X-ray correlations of these sources are fitted based on our model. Some issues related the role of the magnetic fields in state transitions of BHXBs are discussed as follows.

(i) The accretion disk is an ideal site for anchoring the magnetic field. The transport and amplification of the magnetic field are closely related to the accreting plasma from companions of BHXBs, and it provides a reasonable picture for the origin of the magnetic field in BHXBs, and is successful in explaining the main characteristics of LHS of H1743–322 and GX 339–4 in this model. It turns out that the main characteristics of LHS of H1743–322 and GX 339–4 could be interpreted based on this model. As shown in Tables 1 and 2, the truncated radius moves inwards with the transport of the magnetic field in LHS. Thus we think that a stage corresponding to a Magnetically Arrested Disk (MAD) might be a natural outcome that results from concentrating the magnetic field in the inner ADAF (Narayan et al. 2003), giving rise to relativistic transient jets in IMS of BHXBs (Narayan & McClintock 2012; McKinney et al. 2012).

(ii) The state transition of BHXBs is governed by the evolution of the magnetic field configuration. The transition from LHS to HSS can be interpreted by a global magnetic field inversion in the MAD state as argued by Dexter et al. (2014), or by the conversion from a poloidal dominated configuration to a toroidal dominated one as pointed out by King et al. (2012).

(iii) Inspecting Equation (20), we find that the transition X-ray luminosity consists of the contribution from accretion flow ($L_{\rm X}^{II}$) and that from jet ($L_{\rm X}^{I}$). Thus the quite different luminosity during different outbursts of the same source could be fitted based on Equations (5) and (6), provided that $\dot{m}_0$ and B_0 are assigned to different values with the duration time τ for different outbursts.

(iv) The relation between the transition X-ray luminosity and rate-of-change of accretion rate could be derived based on our model, which has been found by Yu & Yan (2009). Differentiating Equation (5), we have

$$(d\dot{m}/dt)_{_{R_{\rm tr}}} = \alpha_{\rm m}\dot{m}_0\tau^{-1}(t/\tau)^{\alpha_{\rm m}-1}, \tag{22}$$

where Equation (22) is valid for the whole rising phase of LHS. Furthermore, we have the accretion rate being related to its rate-of-change by substituting $t = \tau$ into Equation (22), i.e.,

$$(d\dot{m}/dt)_{_{R_{\rm tr}}} = \alpha_{\rm m}\dot{m}_0\tau^{-1}\,. \tag{23}$$

It can be noted that Equation (23) is valid for the transition X-ray luminosity corresponding to IMS, and we can obtain a relation between this luminosity and the rate-of-change of accretion rate by adjusting the related parameters $\alpha_{\rm m}$, $\dot{m}_0$ and τ. Incorporating Equations (5) and (23), we find that the transition luminosity depends not only on the accretion rate, but also on its rate-of-change. This result is consistent with those given by Yu & Yan (2009).

As to the exception that occurred in Cyg X-1, we follow the explanation given in ZCH97: Cyg X-1 probably reflects a change in the relative importance of the energy release in the outer thin disk and the inner ADAF near the BH. This may not require a substantial change in the total accretion rate, but our magnetic model is not applicable to this case.

Frankly speaking, there are a number of problems in this simplified model. First, since the origin and transport of magnetic fields in black hole accretion remains unclear, we suggest that the magnetic flux is carried by the accreting plasma from a companion, which is governed by Equations (5) and (6). Second, also due to a lack of the detailed physical mechanisms related to the origin of magnetic fields, we have to adjust some parameters, such as $\alpha_{\rm m}$ and $\alpha_{_B}$, to fit the main features in the rising phase of LHS of these two sources. Third, only the rising phase of LHS of the two BHXBs, H1743–322 and GX 339–4, is fitted in this paper, but the whole time evolution from quiescent state to LHS, and to IMS is not discussed at all. We shall investigate these issues in our future work.

Acknowledgements This work is supported by the National Basic Research Program of China (973 program, 2009CB824800) and the National Natural Science Foundation of China (Grant Nos. 11173011 and 11403003). We are very grateful to the anonymous referee for his/her helpful suggestions for improving our work.

References

Allured, R., Tomsick, J. A., Kaaret, P., & Yamaoka, K. 2013, ApJ, 774, 135
Belloni, T., Homan, J., Casella, P., et al. 2005, A&A, 440, 207
Blandford, R. D., & Znajek, R. L. 1977, MNRAS, 179, 433
Blandford, R. D., & Payne, D. G. 1982, MNRAS, 199, 883
Blandford, R. D., & Begelman, M. C. 1999, MNRAS, 303, L1
Blum, J. L., Miller, J. M., Cackett, E., et al. 2010, ApJ, 713, 1244
Cabanac, C., Fender, R. P., Dunn, R. J. H., & Körding, E. G. 2009, MNRAS, 396, 1415
Cadolle Bel, M., Ribó, M., Rodriguez, J., et al. 2007, ApJ, 659, 549
Cao, X. 2011, ApJ, 737, 94
Cao, X.-F., Wu, Q., & Dong, A.-J. 2014, ApJ, 788, 52
Corbel, S., & Fender, R. P. 2002, ApJ, 573, L35
Corbel, S., Nowak, M. A., Fender, R. P., Tzioumis, A. K., & Markoff, S. 2003, A&A, 400, 1007
Corbel, S., Fender, R. P., Tomsick, J. A., Tzioumis, A. K., & Tingay, S. 2004, ApJ, 617, 1272
Corbel, S., Coriat, M., Brocksopp, C., et al. 2013, MNRAS, 428, 2500

Coriat, M., Corbel, S., Prat, L., et al. 2011, MNRAS, 414, 677
Cowley, A. P., Schmidtke, P. C., Hutchings, J. B., & Crampton, D. 2002, AJ, 123, 1741
Dexter, J., McKinney, J. C., Markoff, S., & Tchekhovskoy, A. 2014, MNRAS, 440, 2185
Doeleman, S. S., Fish, V. L., Schenck, D. E., et al. 2012, Science, 338, 355
Done, C., Gierliński, M., & Kubota, A. 2007, A&A Rev., 15, 1
Done, C., & Diaz Trigo, M. 2010, MNRAS, 407, 2287
Esin, A. A., McClintock, J. E., & Narayan, R. 1997, ApJ, 489, 865
Esin, A. A., Narayan, R., Cui, W., Grove, J. E., & Zhang, S.-N. 1998, ApJ, 505, 854
Esin, A. A., McClintock, J. E., Drake, J. J., et al. 2001, ApJ, 555, 483
Fender, R. P., Gallo, E., & Jonker, P. G. 2003, MNRAS, 343, L99
Fender, R. P., Belloni, T. M., & Gallo, E. 2004, MNRAS, 355, 1105
Fender, R. P., Russell, D. M., Knigge, C., et al. 2009, MNRAS, 393, 1608
Fender, R., & Belloni, T. 2012, Science, 337, 540
Gallo, E., Fender, R. P., & Pooley, G. G. 2003, MNRAS, 344, 60
Gallo, E., Corbel, S., Fender, R. P., Maccarone, T. J., & Tzioumis, A. K. 2004, MNRAS, 347, L52
Ghosh, P., & Abramowicz, M. A. 1997, MNRAS, 292, 887
Guilet, J., & Ogilvie, G. I. 2013, MNRAS, 430, 822
Hannikainen, D. C., Hunstead, R. W., Campbell-Wilson, D., & Sood, R. K. 1998, A&A, 337, 460
Hawley, J. F., & Balbus, S. A. 2002, ApJ, 573, 738
Heinz, S., & Grimm, H. J. 2005, ApJ, 633, 384
Homan, J., Wijnands, R., van der Klis, M., et al. 2001, ApJS, 132, 377
Homan, J., & Belloni, T. 2005, Ap&SS, 300, 107
Huang, C.-Y., Wu, Q., & Wang, D.-X. 2014, MNRAS, 440, 965 (HWW14)
Hynes, R. I., Steeghs, D., Casares, J., Charles, P. A., & O'Brien, K. 2003, ApJ, 583, L95
Hynes, R. I., Steeghs, D., Casares, J., Charles, P. A., & O'Brien, K. 2004, ApJ, 609, 317
Igumenshchev, I. V. 2009, ApJ, 702, L72
Igumenshchev, I. V., Narayan, R., & Abramowicz, M. A. 2003, ApJ, 592, 1042
Joinet, A., Jourdain, E., Malzac, J., et al. 2005, ApJ, 629, 1008
Jonker, P. G., Miller-Jones, J., Homan, J., et al. 2010, MNRAS, 401, 1255
King, A. L., Miller, J. M., Raymond, J., et al. 2012, ApJ, 746, L20
Kylafis, N. D., & Belloni, T. M. 2015, A&A, 574, A133
Lei, W.-H., Wang, D.-X., & Ma, R.-Y. 2005, ApJ, 619, 420
Lei, W.-H., Wang, D.-X., Zou, Y.-C., & Zhang, L. 2008, ChJAA (Chin. J. Astron. Astrophys.), 8, 404
Li, Y., Gan, Z.-M., & Wang, D.-X. 2010, New Astron., 15, 102
Livio, M., Ogilvie, G. I., & Pringle, J. E. 1999, ApJ, 512, 100
Livio, M. 2002, Nature, 417, 125
Lubow, S. H., Papaloizou, J. C. B., & Pringle, J. E. 1994, MNRAS, 267, 235
MacDonald, D., & Thorne, K. S. 1982, MNRAS, 198, 345
McClintock, J. E., & Remillard, R. A. 2006, Black Hole Binaries, in Compact stellar X-ray sources, eds. W. H. G. Lewin, & M. van der Klis (Cambridge, UK: Cambridge Univ. Press), 157
McClintock, J. E., Remillard, R. A., Rupen, M. P., et al. 2009, ApJ, 698, 1398
McKinney, J. C., Tchekhovskoy, A., & Blandford, R. D. 2012, MNRAS, 423, 3083
Miller, J. M., Fabian, A. C., Reynolds, C. S., et al. 2004, ApJ, 606, L131
Miller, J. M., Homan, J., Steeghs, D., et al. 2006, ApJ, 653, 525
Miller, J. M., Reynolds, C. S., Fabian, A. C., Miniutti, G., & Gallo, L. C. 2009, ApJ, 697, 900
Miller, J. M., Raymond, J., Fabian, A. C., et al. 2012, ApJ, 759, L6
Miyamoto, S., Kitamoto, S., Hayashida, K., & Egoshi, W. 1995, ApJ, 442, L13
Motta, S., Muñoz-Darias, T., & Belloni, T. 2010, MNRAS, 408, 1796
Muñoz-Darias, T., Casares, J., & Martínez-Pais, I. G. 2008, MNRAS, 385, 2205
Nandi, A., Debnath, D., Mandal, S., & Chakrabarti, S. K. 2012, A&A, 542, A56
Narayan, R., & Yi, I. 1994, ApJ, 428, L13
Narayan, R., & Yi, I. 1995, ApJ, 444, 231
Narayan, R., Igumenshchev, I. V., & Abramowicz, M. A. 2000, ApJ, 539, 798
Narayan, R., Igumenshchev, I. V., & Abramowicz, M. A. 2003, PASJ, 55, L69
Narayan, R., & McClintock, J. E. 2012, MNRAS, 419, L69
Paczyński, B. 1971, ARA&A, 9, 183
Plant, D. S., Fender, R. P., Ponti, G., Muñoz-Darias, T., & Coriat, M. 2014, MNRAS, 442, 1767
Quataert, E., & Gruzinov, A. 2000, ApJ, 539, 809
Ratti, E. M., Jonker, P. G., Miller-Jones, J. C. A., et al. 2012, MNRAS, 423, 2656
Reis, R. C., Fabian, A. C., Ross, R. R., et al. 2008, MNRAS, 387, 1489
Remillard, R. A., McClintock, J. E., Orosz, J. A., & Levine, A. M. 2006, ApJ, 637, 1002
Sikora, M., & Begelman, M. C. 2013, ApJ, 764, L24
Soleri, P., Fender, R., Tudose, V., et al. 2010, MNRAS, 406, 1471
Spruit, H. C., & Uzdensky, D. A. 2005, ApJ, 629, 960
Spruit, H. C. 2010, in Lecture Notes in Physics, Berlin Springer Verlag, 794, ed. T. Belloni, 233 (arXiv: 0804.3096) (Berlin: Springer Verlag)
Sriram, K., Agrawal, V. K., & Raghurama Rao, A. 2009, RAA (Research in Astronomy and Astrophysics), 9, 901
Stone, J. M., Pringle, J. E., & Begelman, M. C. 1999, MNRAS, 310, 1002
Tomsick, J. A., Yamaoka, K., Corbel, S., et al. 2009, ApJ, 707, L87

Wu, Q., & Cao, X. 2006, PASP, 118, 1098
Wu, Q., & Gu, M. 2008, ApJ, 682, 212
Wu, Q., Cao, X., & Wang, D.-X. 2011, ApJ, 735, 50
Wu, Q., Yan, H., & Yi, Z. 2013, MNRAS, 436, 1278
Yu, W., van der Klis, M., & Fender, R. 2004, ApJ, 611, L121
Yu, W., & Yan, Z. 2009, ApJ, 701, 1940
Yuan, F. 1999, ApJ, 521, L55
Yuan, F. 2001, MNRAS, 324, 119
Yuan, F., Cui, W., & Narayan, R. 2005, ApJ, 620, 905
Yuan, F., Ma, R., & Narayan, R. 2008, ApJ, 679, 984 (YMN08)
Yuan, F., & Narayan, R. 2014, ARA&A, 52, 529
Zdziarski, A. A., Gierliński, M., Mikołajewska, J., et al. 2004, MNRAS, 351, 791
Zhang, S. N., Cui, W., Harmon, B. A., et al. 1997, ApJ, 477, L95 (ZCH97)